SECOND LAW ANALYSIS OF LAMINAR FORCED CONVECTION IN A ROTATING CURVED DUCT

by

Seyed Esmail RAZAVI[a], Hosseinali SOLTANIPOUR[b*], and Parisa CHOUPANI[a]

[a] Department of Mechanical Engineering, University of Tabriz, Tabriz, Iran
[b] Department of Mechanical Engineering, Urmia University of Technology, Urmia, Iran

Original scientific paper
DOI:10.2298/TSCI120606034R

In this paper, flow characteristics, heat transfer and entropy generation in a rotating curved duct are studied numerically. The continuity, Navier-Stokes and energy equations are solved using control volume method. The effects of Dean number, non-dimensional wall heat flux, and force ratio (the ratio of Coriolis to centrifugal forces) on the entropy generation due to friction and heat transfer irreversibility and also overall entropy generation are presented. Optimal thermal operating conditions (based on dimensionless parameters) are determined from the viewpoint of thermodynamics second law. The comparison of numerical results at different force ratios indicates that for any fixed Dean number or non-dimensional heat flux, the minimal frictional entropy generation occurs when the Coriolis and centrifugal forces have the same value but in the opposite direction. For a specific non-dimensional heat flux, there is a force ratio with maximum heat transfer irreversibility which depends on Dean number. Based on optimal analysis, the optimal force ratio with minimal total entropy generation depends on heat flux and Dean number.

Key words: *entropy generation, laminar flow, Navier-Stokes equations, Dean number, force ratio, irreversibility, curved duct*

Introduction

Fluid flow in rotating curved ducts has various applications in engineering systems. Examples where this type of flow occurs are lubricants in internal combustion engine passages, fluids in cooling systems, air flow in turbo-machinery passages such as gas turbines, electric generators, rotating heat exchangers, *etc*.

Because of curvature and rotation, fluid flow in rotating curved duct is influenced by the centrifugal and Coriolis forces. The interaction of these forces makes the flow structure to be complicated. There are numerous published papers related to analysis of flow and thermal fields in stationary curved ducts with different cross-sections. For instance, Chandratilleke [1] performed experiments and Chandratilleke and Nursubyakto [2] used both experimental and numerical methods to study the secondary flow and convective heat transfer in curved rectangular ducts. They analyzed the effects of Dean number and duct aspect ratio on the heat transfer coefficient and flow field. Boutabaa *et al.* [3] numerically studied developing secondary flows of Newtonian and viscoelastic fluids through a curved duct of square cross-section.

In the case of flow in rotating curved ducts, Zhang *et al.* [4] studied numerically the combined effect of the Coriolis and centrifugal forces. The effects of force ratio and as-

* Corresponding author; e-mail: h.soltanipour@gmail.com

pect ratio of cross-section on the characteristics of secondary and main flow and also friction factor were considered. Zhang *et al.* [5] used the perturbation method to study the flow in a rotating annular pipe. They investigated the characteristics of the secondary and the axial flows in detail.

Papa *et al.* [6] obtained numerical results for developing laminar flow in ducts having either circular or square cross-sections with a 180-degree bend rotating positively or negatively about an axis parallel to the axis of curvature of the duct. They showed that rotation causes the secondary flow to occur in ducts of any geometry. Laminar flow and heat transfer in a rotating U-shaped duct with square cross-section was studied by Nobari *et al.* [7]. They found that the maximum heat transfer occurs when duct rotates about an axis parallel to the axis of duct curvature, at which both the Coriolis and the centrifugal forces intensify each other. Ma *et al.* [8] investigated three-dimensional laminar flow in the entrance region of rotating curved pipes. They indicated that rotation greatly influences the flow structure and friction factor. They concluded that average friction factor and the intensity of secondary flow have drastic decrease near the entrance.

Recently, the second law of thermodynamics has been used to optimize thermal systems. Based on the concept of efficient exergy and minimal entropy generation principal, optimal design of thermal systems has been widely proposed. Bejan [9] presented the methodology of computing entropy generation due to heat and fluid flow and entropy generation minimization [10]. The amount and distribution of entropy generation in flow field is a substantial point in design of thermal systems. Accordingly, the effects of geometrical parameters, flow and boundary conditions and thermo-physical properties of working fluid on entropy generation in conventional and micro-channels have received continuous attention [11-16].

In the stationary rectangular curved ducts, Ko and Ting [17] studied laminar flow and heat transfer from viewpoint second law of thermodynamics. Based on the minimal entropy generation principle, they presented the optimal design parameters such as the aspect ratio of cross-section, Dean number and external heat flux. Moreover, Ko [18, 19] investigated the effects of rib size, number and position of ribs on the entropy generation in ribbed curved ducts. More recently, Amani and Nobari [20, 21] analyzed the entropy generation and thermodynamic optimization in the entrance region of curved pipes for both constant wall temperature and heat flux boundary conditions. They studied the effects of important parameters such as Reynolds number and curvature ratio on the entropy generation through heat transfer and frictional irreversibilities.

Most of the previous investigations on flow in rotating curved ducts are restricted to the analysis based on the first law of thermodynamics and to our knowledge, there are no studies based on the second law. The aim of the present paper is to investigate the entropy generation due to laminar forced convection in a rotating curved duct with square cross-section. The influences of non-dimensional wall heat flux, Dean number and force ratio on the entropy generation are analyzed.

Problem description

The problem is 3-D, steady, incompressible and forced laminar convection of air flowing inside a curved square duct having the side length and curvature radius of H and R, respectively. In this study, the curvature ratio (H/R) is equal to 0.2. As shown in fig.1, the duct rotates around z-axis with constant angular velocity ω. According to the figure, the Cartesian co-ordinate system is used in this work, which its origin is taken at the center "O" of the curved duct.

The Reynolds and Dean numbers, force ratio, and non-dimensional wall heat flux for the current problem are defined as:

$$\mathrm{Re} = \frac{V_{\mathrm{in}} H}{\nu} \tag{1}$$

$$\mathrm{De} = \mathrm{Re}\sqrt{\frac{H}{R}} \tag{2}$$

$$F = \frac{\omega R}{V_{\mathrm{in}}} \tag{3}$$

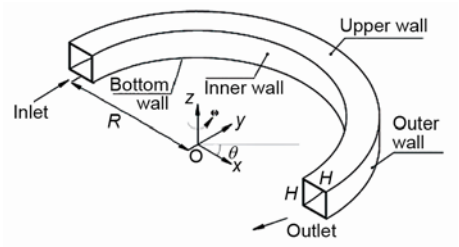

Figure 1. Geometry of curved duct and co-ordinate system

$$q^{*} = \frac{q'' H}{k T_{\mathrm{in}}} \tag{4}$$

where V_{in} and T_{in} are the average inlet velocity and temperature, and q'' is the external wall heat flux. The parameter F is used by Ishigaki for first time [22, 23], as the ratio of Coriolis to centrifugal forces. The $F < 0$ represents negative rotation in which Coriolis and centrifugal forces are in the opposite directions; while $F > 0$ is positive rotation in which two mentioned forces have the same directions and, finally, $F = 0$ deals with stationary curved duct (without rotation). There is not exact information on the critical values of Reynolds (or Dean) number and Force ratio for flow in a rotating curved duct in open publications. Therefore, for ensuring that all studied cases are laminar flows, the calculation is carried out for Dean number ranging 100-500 and force ratio ranging from –2 to 2. Three different values of dimensionless wall heat flux, *i. e.*, $q^{*} = 0.007$, 0.014, and 0.028 are considered to investigate the effects of wall heat flux on entropy generation.

Governing equations and boundary conditions

Using the following non-dimensional parameters:

$$x^{*} = \frac{x}{H}, \quad y^{*} = \frac{y}{H}, \quad z^{*} = \frac{z}{H}, \quad \vec{\mathrm{V}}^{*} = \frac{\vec{\mathrm{V}}}{V_{\mathrm{in}}}, \quad P^{*} = \frac{P}{\rho V_{\mathrm{in}}^{2}},$$

$$T^{*} = \frac{T - T_{\mathrm{in}}}{T_{\mathrm{in}}}, \quad \vec{\mathrm{a}}^{*} = \frac{\vec{\mathrm{a}}\, H}{V_{\mathrm{in}}^{2}}, \quad \vec{\mathrm{r}}^{*} = \frac{\vec{\mathrm{r}}}{H}, \quad \nabla^{*} = H\nabla, \quad \omega^{*} = \frac{\omega H}{V_{\mathrm{in}}}, \quad \mathrm{Pr} = \frac{\nu}{\alpha}$$

The dimensionless continuity, Navier-Stokes and energy equations in the Cartesian co-ordinate system are:

$$\nabla^{*} \vec{\mathrm{V}}^{*} = 0 \tag{5}$$

$$(\vec{\mathrm{V}}^{*} \nabla^{*} \vec{\mathrm{V}}^{*}) = -\nabla^{*} P^{*} + \frac{1}{\mathrm{Re}} \nabla^{*2} \vec{\mathrm{V}}^{*} + \vec{\mathrm{a}}^{*} \tag{6}$$

$$\vec{\mathrm{V}}^{*} \nabla^{*} T^{*} = \frac{1}{\mathrm{Re}\,\mathrm{Pr}} \nabla^{*2} T^{*} \tag{7}$$

where the starred variables are dimensionless ones, P denotes the pressure, T – the temperature, and $\vec{\mathrm{V}}$ and $\vec{\mathrm{r}}$ are the velocity and position vectors, respectively. The centrifugal and Coriolis resultant acceleration in dimensionless vector form is:

$$\vec{\mathrm{a}}^* = -\vec{\omega}^* \times \vec{\omega}^* \times \vec{\mathrm{r}}^* - 2\vec{\omega}^* \times \vec{\mathrm{V}}^* \tag{8}$$

The non-linear governing equations of the problem are subjected to following boundary conditions.

At the duct inlet, uniform axial velocity (V_{in}) and temperature (T_{in}) are specified.

$$V_x^* = V_z^* = 0, \quad V_y^* = 1, \quad T^* = 0 \tag{9}$$

At the walls, no-slip condition is used for velocity components. The constant heat flux is specified only on the outer wall ($q^* = -\nabla^* T^*$), whereas other walls of the curved duct are adiabatic ($-\nabla^* T^* = 0$). At the outlet, fully developed boundary condition is adopted.

After solving the governing equations, the volumetric entropy generation due to the heat transfer irreversibility, S_T''', fluid frictional irreversibility, S_f''', and total entropy generation, S_{gen}''', are expressed as [9]:

$$S_f''' = \frac{\mu}{T}\varphi \tag{10}$$

$$S_T''' = \frac{k}{T^2}\left(|\nabla T|\right)^2 \tag{11}$$

$$S_{\mathrm{gen}}''' = S_f''' + S_T''' \tag{12}$$

where, φ is the viscous dissipation function given by:

$$\varphi = 2\left[\left(\frac{\partial V_x}{\partial x}\right)^2 + \left(\frac{\partial V_y}{\partial y}\right)^2 + \left(\frac{\partial V_z}{\partial z}\right)^2\right] + \left(\frac{\partial V_x}{\partial y} + \frac{\partial V_y}{\partial x}\right)^2 + \left(\frac{\partial V_y}{\partial z} + \frac{\partial V_z}{\partial y}\right)^2 + \left(\frac{\partial V_x}{\partial z} + \frac{\partial V_z}{\partial x}\right)^2 - \frac{2}{3}(\vec{\nabla}\vec{V})^2 \tag{13}$$

The Bejan number describes the contribution of heat transfer entropy generation on overall entropy generation, which defined as:

$$\mathrm{Be} = \frac{S_T'''}{S_{\mathrm{gen}}'''} \tag{14}$$

Numerical method and grid system

Governing eqs. (5)-(7) are solved by control volume based SIMPLE approach [24] with first-order upwind scheme for the convection and central differencing scheme for the diffusion terms on a staggered grid. A convergence criteria of 10^{-6} is used for all calculations.

In order to ensure grid independency, three grid sizes are submitted to an extensive testing of results. Comparison of different grid system results (for the average friction factor and Nusselt number in the case De = 500, $q^* = 0.028$, and $F = -2$) is shown in tab. 1. It is observed that the grid system with 40 × 40 × 80 nodal points (40 × 40 on the cross-sectional

plane and 80 nodes along the axial direction) has satisfactory independency with respect to the number of elements used. Consequently, aforementioned grid is adopted for different flow conditions.

Table 1. The grid independency study

Grid size	$\overline{C}_f$	$\overline{\mathrm{Nu}}$
20 × 20 × 50	0.035	18.13
40 × 40 × 80	0.037	18.75
45 × 45 × 100	0.037	18.84

Validation of the present simulation

To examine the accuracy of present results, we first compared numerical results with experimental data of Hille *et al.* [25]. The comparison is illustrated in fig. 2, where in, the variation of axial velocity at two cross-sectional planes (*i. e.*, $\theta = 90°$ and 144°) for flow inside a curved duct as a function of distance along the radial location (at $z = 0$) is presented. As shown in fig. 2, the obtained distributions of axial velocity demonstrate good agreement with the measured data.

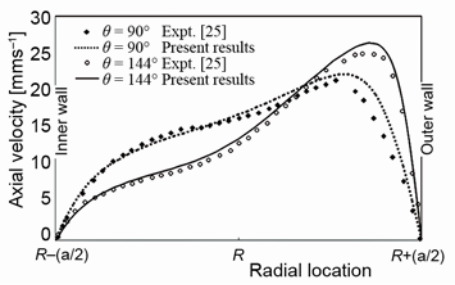

Figure 2. Axial velocity as a function of the radial location at the midplane of cross--section for De = 226 and $F = 0$

Another comparison is made with the numerical results of Papadopoulos *et al.* [26] for developing flow through a stationary curved duct with isothermal boundary condition. The average Nusselt number *vs.* Dean number is depicted in fig. 3. It is observed that the maximum deviation of 2.75% appears for the Nusselt number at De = 175.

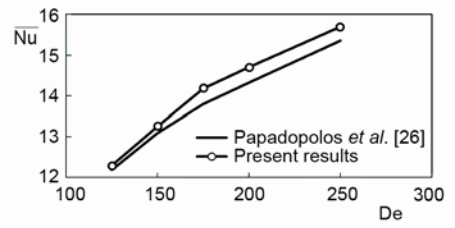

Figure 3. Comparison of present results with that of Papadopoulos *et al.* [26]

Results and discussions

To analyze the combined effects of rotation and curvature on the flow field, velocity vectors at different force ratios on $\theta = 45°$ are shown in fig. 4. In this figure, outer wall is at left-hand side (LHS) and inner wall is at right-hand side (RHS). For the stationary case ($F = 0$), two pairs of vortices are formed; one pair is located near the outer wall, and the another pair composed of two vortices with long and narrow shape distribution adjacent to the upper and lower walls. By increasing the force ratio in the positive direction, the secondary flow is strengthened because the Coriolis force has the same direction as the centrifugal force. The effect of increasing F is similar to increasing Dean number, and as a result the vortices gradually become larger. This trend continues up to $F = 1$ however, at $F = 2$, another vortex pair is formed on the corners of inner wall.

For counter-rotating flows ($F < 0$), the Coriolis and the centrifugal forces are in the opposite direction. For example, at $F = –0.5$ the centrifugal force is dominated and as shown in figure, the vortices near the outer wall disappear whereas vortex structure near the upper and lower walls remain almost unchanged. This behavior is similar to flow pattern in a stationary curved duct at low Dean numbers. At $F = –1$, both forces have the comparable order of magnitude, thus a complicated structure of the secondary flow composed of four vortices is observed. When $|F|$ increases in negative direction, the vortices near upper and lower walls rotate in inverse direction and gradually become larger, and finally at $F = –2$, another vortex pair is formed near the inner wall.

Figure 5 shows the non-dimensional axial velocity ($V_{\mathrm{axial}}/V_{\mathrm{in}}$) contours for different force ratios.

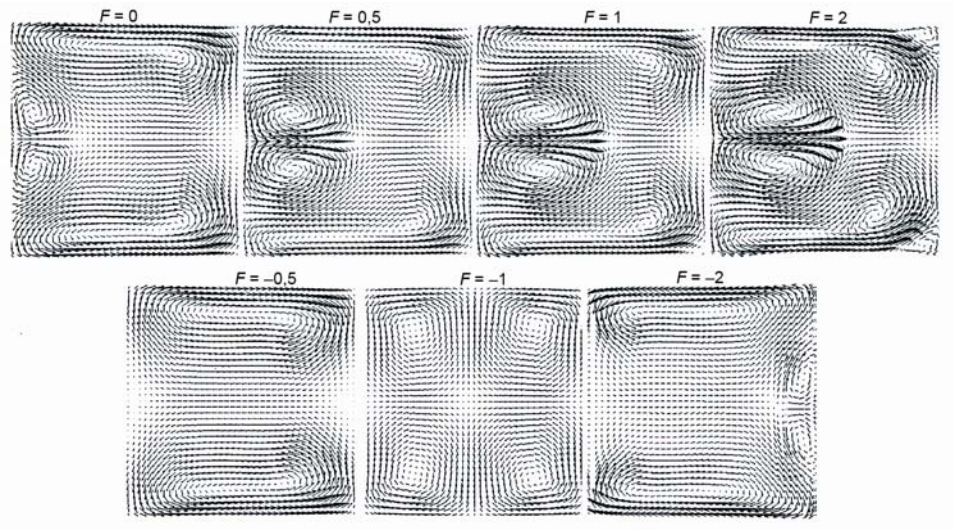

Figure 4. Velocity vectors at θ = 45°, De = 500, q^* = 0.014. Outer wall is at LHS, and inner wall is at RHS

At $F = 0$, the curvature of the duct makes the higher velocity is tend to outer wall due to the centrifugal effects and by increasing the force ratio in positive direction, the fluid with high velocity transfers toward outer wall due to the Coriolis effects. When the strengths of two secondary flows have nearly the same magnitude, and they coexist in the cross-section, as the case $F = -1$, the effects of the two opposite secondary flows on the primary flow neutralize each other and the distributions of axial flow are similar to uniform flow. As F decreases further, the Coriolis force becomes dominating and consequently, centrifugal force-driven secondary vortex disappears and the fluid velocity near the inner wall increases.

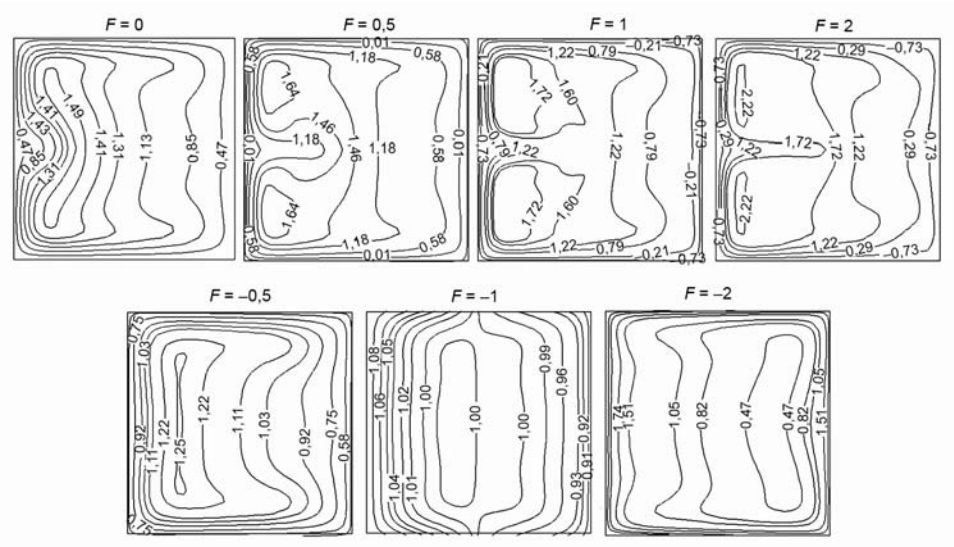

Figure 5. Non-dimensional axial velocity contours, at θ = 45°, q^* = 0.014, De = 500. Outer wall is at LHS, and inner wall is at RHS

The non-dimensional temperature contours are depicted in fig. 6. Obviously, the remarkable temperature rise occurs in a region near the outer wall, which is exposed to the external heat flux. As F increases in the positive direction, because of strengthened secondary flow, the hot fluid near the outer wall mixes to low temperature in central regions, and as a result, high temperature zone penetrates to center of cross-section. For the negative rotation and small $|F|$, fluid with high temperature zone concentrated near the outer wall. As $|F|$ more increases, because of intensified secondary motion in reverse direction, high temperature flow moves toward the inner wall.

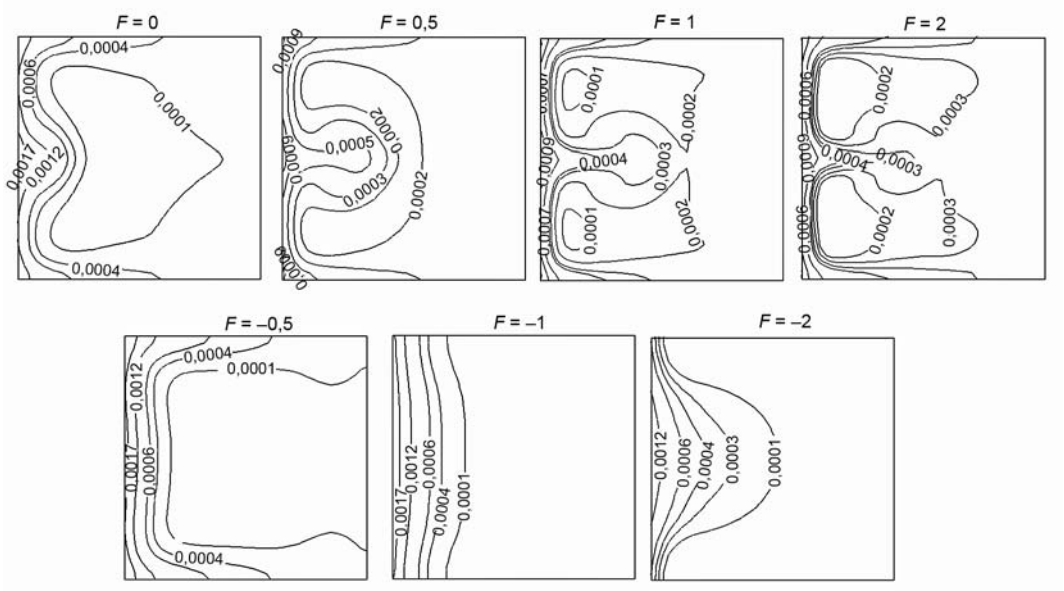

Figure 6. Non-dimensional temperature contours at θ = 45°, q^* = 0.014, De = 500. Outer wall is at LHS, and inner wall is at RHS

The distribution of entropy generation due to friction, heat transfer and total entropy generation at different force ratios are presented in figs. 7-9.

As shown in fig. 7, the remarkable values of S_f''' observed only in the regions adjacent to the duct walls because of the high velocity gradient in these regions. The increase of F in the positive direction cause to increase of S_f''', which is attributed to the more fluid friction. For negative rotation, by increasing F, S_f''' decreases and $F = -1$ has negligible values of S_f''' compared to $F = -0.5$. Moreover, for $F = -2$, the value of S_f''', near the inner wall is higher than corresponding values adjacent to outer wall.

The distributions of S_T''' for various force ratios are shown in fig. 8. It is clear that the major values of S_T''' concentrates near the outer wall. As force ratio increase in positive direction, the values of S_T''' near the outer wall decreases. It is observed that S_T''' values in the positive rotation have small values compared to negative rotation.

The distribution of overall entropy generation in cross-sectional plane is illustrated in fig. 9. For all cases considered here, the significant values of S_{gen}''' is detected near the duct walls. Besides, the highest values of S_{gen}''' is found near outer wall which has both irreversibilites of fluid friction and heat transfer.

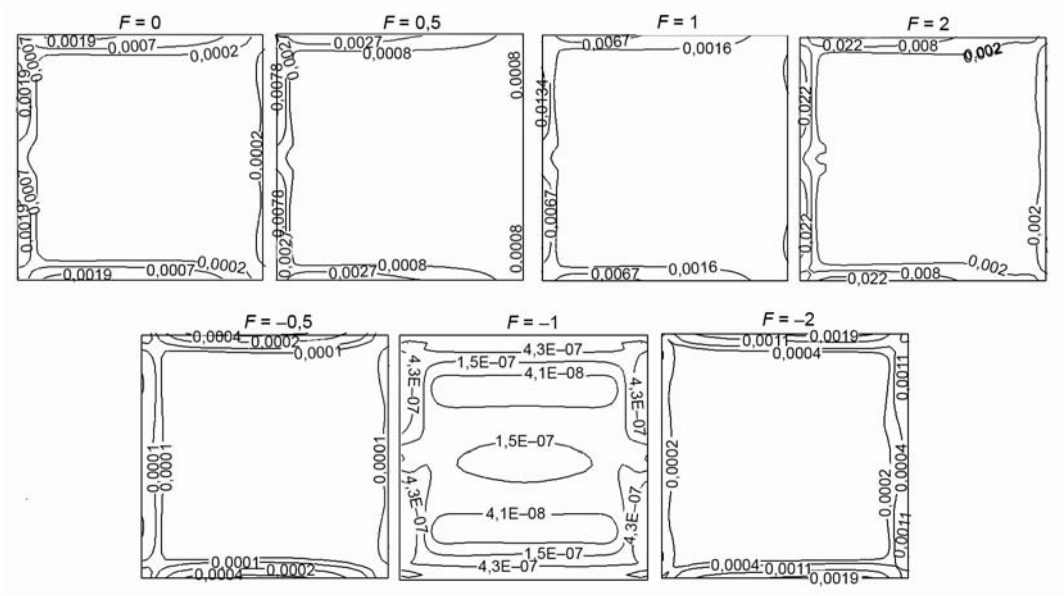

Figure 7. Contours of volumetric entropy generation due to friction, S_f''' at θ = 45°, q^* = 0.014, De = 500. Outer wall is at LHS, and inner wall is at RHS

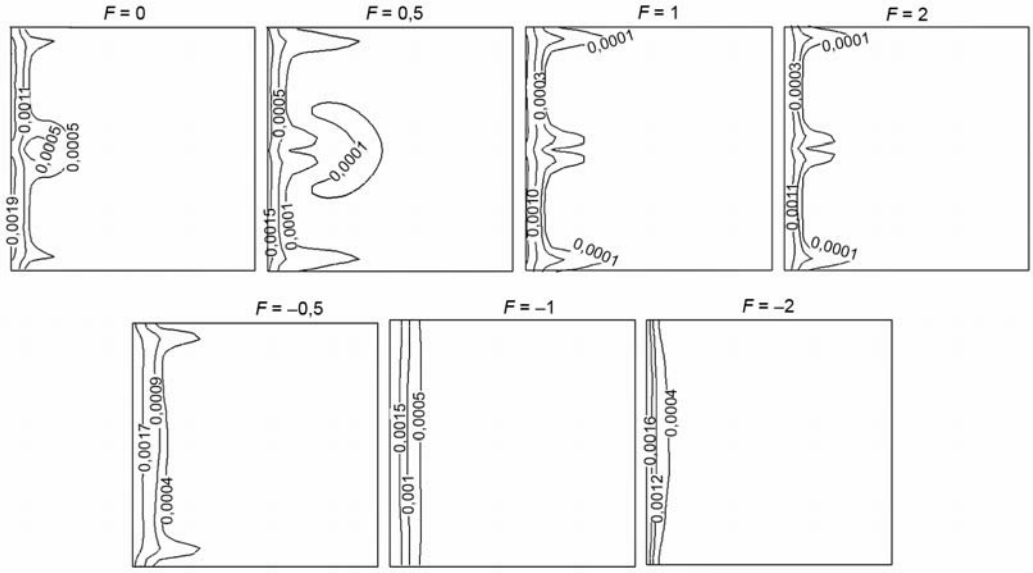

Figure 8. Contours of volumetric entropy generation due to heat transfer, S_T''' at θ = 45°, q^* = 0.014, De = 500. Outer wall is at LHS, and inner wall is at RHS

In order to determine the contribution of the heat transfer and frictional irreversibilites in resultant entropy generation, the contours of Bejan number for different force ratios are plotted in fig. 10. For $F > 0$, Bejan number near the outer wall is less than 0.5 that indicates frictional irreversibility portion in overall entropy generation is dominated. In

contrast, for negative rotation, Bejan number adjacent to outer wall is nearly unity. Which indicates that S_T''' is the dominate term in total entropy generation.

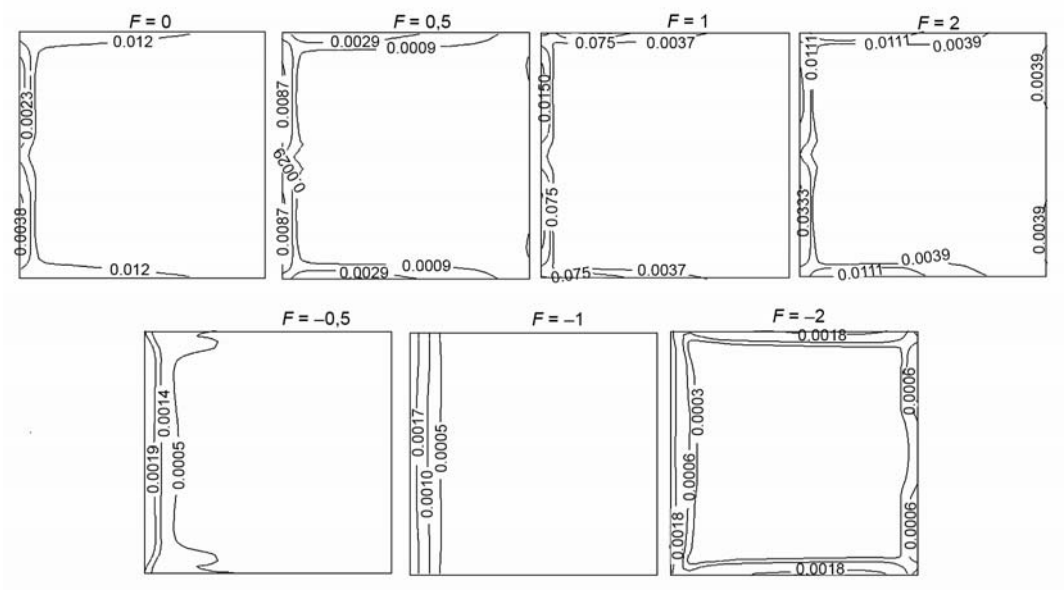

Figure 9. Contours of volumetric overall entropy generation, S_{gen}''' at θ = 45°, q^* = 0.014, De = 500. Outer wall is at LHS, and inner wall is at RHS

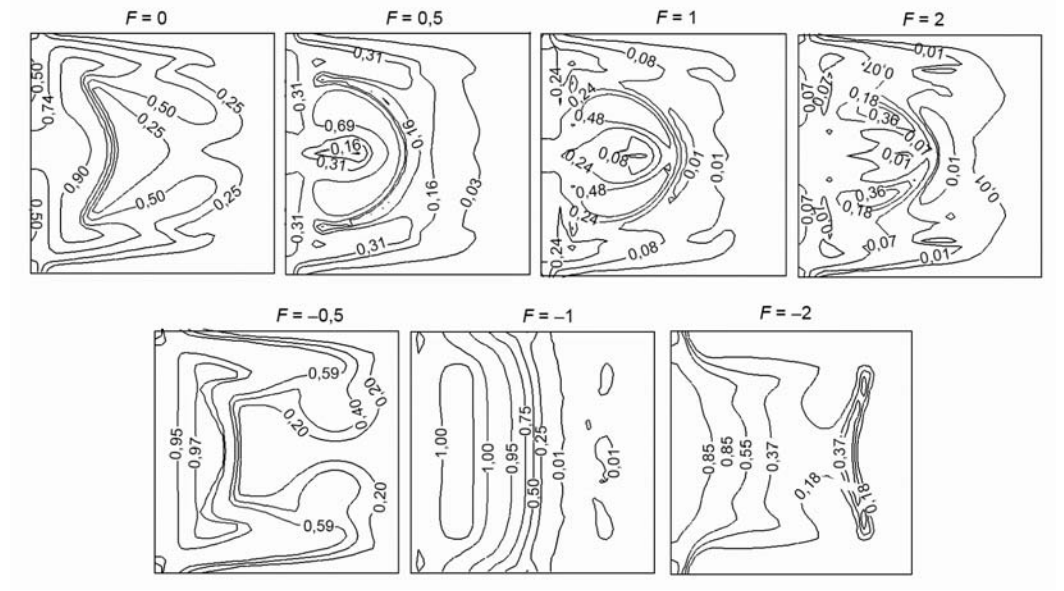

Figure 10. Contours of Bejan number, Be, at θ = 45°, q^* = 0.014, De = 500. Outer wall is at LHS, and inner wall is at RHS

The non-dimensional entropy generation rate, S_f^*, S_T^*, and S_{gen}^* in the whole curved duct are defined by [27]:

$$S_f^* = \frac{\int_V S_f''' \, \mathrm{d}V}{\frac{\dot{Q}}{T_{\text{in}}}} \tag{16}$$

$$S_T^* = \frac{\int_V S_T''' \, \mathrm{d}V}{\frac{\dot{Q}}{T_{\text{in}}}} \tag{17}$$

$$S_{\text{gen}}^* = \frac{\int_V S_{\text{gen}}''' \, \mathrm{d}V}{\frac{\dot{Q}}{T_{\text{in}}}} \tag{18}$$

where $\dot{Q}$ is the heat transfer rate from the outer wall. The variation of frictional entropy generation *vs.* force ratio at different Dean numbers is shown in fig. 11. At specified force ratio, the value of S_f^* increases with the rise of Dean number. This is due to the fact, that frictional irreversibility is related to velocity gradients, which is larger at high Dean numbers. Another feature of fig. 11 is that in the case of positive rotation, S_f^* increases as F rises. For the considered values of F, the case with $F = -1$, has the minimum value of S_f^*.

Figure 12 indicates the values of entropy generation due to heat transfer irreversibility for force ratio ranging from –2 to 2 at various Dean numbers. One can see that regardless of value of Dean number, S_T^* values for any positive F, is less than corresponding value for negative F. For De = 200 and 300, the maximum value of S_T^* occurs in $F = 0$, while corresponding value for De = 500 appears in $F = -0.5$. Furthermore, for specified value of force ratio, S_T^* decreases with the increase of Dean number.

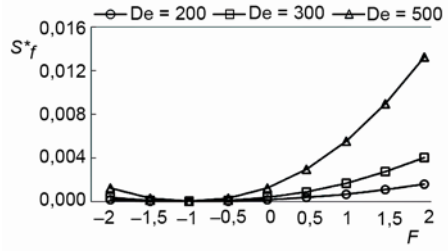

Figure 11. Variation of S_f^* with F at $q^* = 0.014$

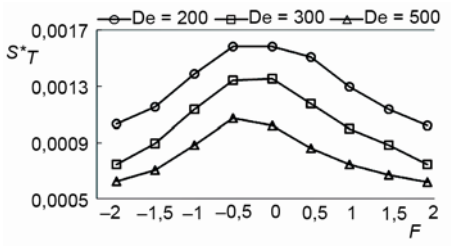

Figure 12. Variation of S_T^* with F at $q^* = 0.014$

Figure 13 shows the variation of S_{gen}^* with F for different Dean numbers. The figure clarifies that S_{gen}^* is not monotonically related to F and De. At De = 300 and De = 500, the optimal F with minimal S_{gen}^* are –1.5 and –1, respectively.

Figure 14 illustrates the variation of Bejan number against F for various Dean numbers. For all Dean numbers considered here, the maximum value of Bejan number is found at $F = -1$. Moreover, for specified F, Bejan number decreases by increasing Dean number.

The effects of non-dimensional wall heat flux on S_f^*, S_T^*, and S_{gen}^* at De = 300 are shown in figs. 15, 16, and 17, respectively. A clear trend can be found from fig. 15 that for all force ratios, S_f^* decreases as q^* increases. Because, there is $\dot{Q}/T_{\text{in}}$ term in the denominator of S_f^*.

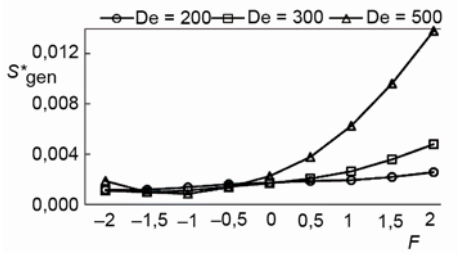

Figure 13. Variation of S^*_{gen} with F at q^* = 0.014

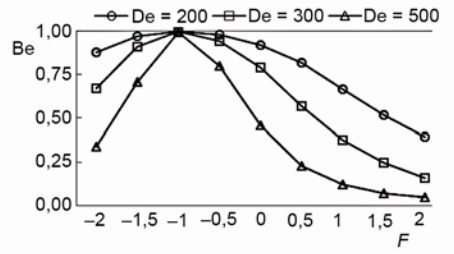

Figure 14. Variation of Bejan number with F at q^* = 0.014

Figure 16 shows the variation of S^*_T with F at De = 300 and various q^*. It is clear that the irreversibility due to the heat transfer increases with rising of q^*. For all cases with different q^*, S^*_T reaches its maximum value at $F = 0$.

Figure 17 shows the variation of S^*_{gen} with F at different q^*. From this figure it is evident that for cases with q^* = 0.007 and q^* = 0.014, S^*_{gen} has the minimum value at $F = -1$ and $F = -1.5$, respectively.

Conclusions

Laminar forced convection and entropy generation in a curved duct, which rotates about an axis parallel to the axis of duct curvature, is investigated by numerical methods. The effects of three different parameters *i. e.*, Dean numbers, non-dimensional wall heat flux, and force ratio on entropy generation is presented. Results show that the formation of secondary flow depends strongly upon duct rotation. Vorticity can be generated by the Coriolis force as well as centrifugal force. For positive rotation, both the Coriolis and the centrifugal forces have the same direction and augment each other. Therefore, the secondary flow strengthened and the high velocity zone more pushed to outer wall. Analysis of entropy generation indicates that at positive rotation, the increase of force ratio cause to increase of entropy generation due to friction and decrease of entropy generation due to heat transfer. Moreover, for specific force ratio, by increasing of Dean number, entropy generation due to friction rises while entropy generation due to heat transfer decreases. Regardless of the value of Dean number, entropy generation due to heat trans-

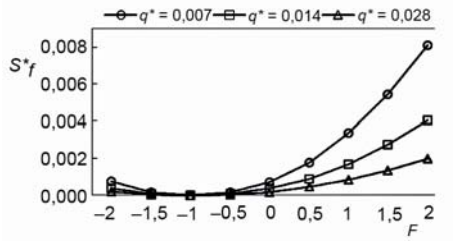

Figure 15. Effects of q^* on entropy generation induced by friction (S^*_f) at De = 300

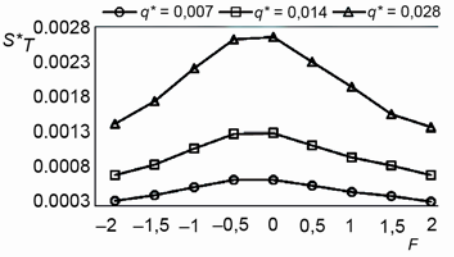

Figure 16. Effects of q^* on entropy generation induced by heat transfer (S^*_T) at De = 300

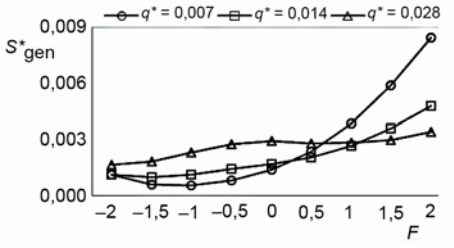

Figure 17. Effects of q^* on total entropy generation (S^*_{gen}) at De = 300

fer for any positive rotation, is less than corresponding value for negative rotation. Numerical results reveal that for specific force ratio, increase of non-dimensional wall heat flux cause to decrease of entropy generation due to friction and increase of entropy generation due to heat transfer. Based on the second law of thermodynamics and minimal entropy generation principle, the optimal force ratio depends on non-dimensional wall heat flux and Dean number.

Nomenclature

$\bar{C}_f$ – average friction factor $(= 2\bar{\tau}_w/\rho V_{in}^2)$, [–]
$\bar{h}$ – average heat transfer coefficient, [$Wm^{-2}K^{-1}$]
k – thermal conductivity, [$Wm^{-1}K^{-1}$]
$\overline{Nu}$ – average Nusselt number $(= \bar{h}H/k)$, [–]
V_x, V_y, V_z – velocity components in x-, y- and z-directions, [ms^{-1}]
V_{axial} – axial velocity, [ms^{-1}]

Greek symbols

α – thermal diffusivity, [m^2s^{-1}]
μ – dynamic viscosity, [Pa·s]
ν – kinematic viscosity, [m^2s^{-1}]
ρ – density, [kgm^{-3}]
$\bar{\tau}_w$ – average wall shear stress, [Pa]

References

[1] Chandratilleke, T. T., Secondary Flow Characteristics and Convective Heat Transfer in a Curved Rectangular Duct with External Heating, *Proceedings,* 5th World Conference on Experimental Heat Transfer, Fluid Mechanics and Thermodynamics, ExHFT-5, Thessaloniki, Greece, 2001, pp. 24-28
[2] Chandratilleke, T. T., Nursubyakto, Numerical Prediction of Secondary Flow and Convective Heat Transfer in Externally Heated Curved Rectangular Ducts, *International Journal of Thermal Sciences*, *42* (2003), 2, pp. 187-198
[3] Boutabaa, M., *et al.*, Numerical Study of Dean Vortices in Developing Newtonian and Viscoelastic Flows through a Curved Duct of Square Cross-Section, *C. R. Mecanique*, *337* (2009), 1, pp. 40-47
[4] Zhang, J. S., *et al*., Fluid Flow in a Rotating Curved Rectangular Duct, *International Journal of Heat and Fluid Flow*, *22* (2001), 6, pp. 583-592
[5] Zhang, B. Z., *et al.*, The Perturbation Solutions of the Flow in a Curved Rotating Annular Pipe, *Journal of Hydrodynamics Ser. B*, *13* (2001), 1, pp. 75-80
[6] Papa, F., *et al.*, Numerical Calculation of Developing Laminar Flow in Rotating Ducts with a 180-deg Bend, *International Journal Numerical Methods for Heat & Fluid Flow*, *12* (2002), 7, pp. 780-799
[7] Nobari, M. R. H., *et al*., A Numerical Investigation of Flow and Heat Transfer in Rotating U-Shaped Square Ducts, *International Journal of Thermal Sciences*, *48* (2009), 3, pp. 590-601
[8] Ma, J. F, *et al.*, Laminar Developing Flow in the Entrance Region of Rotating Curved Pipes, *Journal of Hydrodynamics Ser. B*, *18* (2006), 4, pp. 418-423
[9] Bejan, A., *Entropy Generation through Heat and Fluid Flow*, John Wiley & Sons, New York, USA, 1982
[10] Bejan, A., *Entropy Generation Minimization*, CRC Press, Boca Raton, Fla., USA, 1996
[11] Guo, J., *et al*., Second Law Analysis of Curved Rectangular Channels, *International Journal of Thermal Sciences, 50* (2011), 5, pp. 760-768
[12] Guo, J., *et al.*, The Effect of Temperature-Dependent Viscosity on Entropy Generation in Curved Square Microchannel, *Chemical Engineering and Processing: Process Intensification, 52* (2012), Feb., pp. 85-91
[13] Jarungthammachote, S., Entropy Generation Analysis for Fully Developed Laminar Convection in Hexagonal Duct Subjected to Constant Heat Flux, *Energy*, *35* (2010), 12, pp. 5374-5379
[14] Chakraborty, S., Ray, S., Performance Optimization of Laminar Fully Developed Flow through Square Ducts with Rounded Corners, *International Journal of Thermal Sciences*, *50* (2011), 12, pp. 2522-2535
[15] Esfahani, J. A., Shahabi, P. B., Effect of Non-Uniform Heating on Entropy Generation for the Laminar Developing Pipe Flow of a High Prandtl Number Fluid, *Energy Conversion and Management*, *51* (2010), 11, pp. 2087-2097
[16] Nourollahi, M., *et al*., Numerical Study of Mixed Convection and Entropy Generation in the Poiseulle--Benard Channel in Different Angles, *Thermal Science*, *14* (2010), 2, pp. 329-340
[17] Ko, T. H., Ting, K., Entropy Generation and Optimal Analysis for Laminar Forced Convection in Curved Rectangular Ducts: A Numerical Study, *International Journal of Thermal Sciences*, *45* (2006), 2, pp. 138-150

[18] Ko, T. H., Numerical Investigation on Laminar Forced Convection and Entropy Generation in a Curved Rectangular Duct with Longitudinal Ribs Mounted on the Heated Wall, *International Journal of Thermal Science, 45* (2006), 4, pp. 390-404
[19] Ko, T. H., A Numerical Study on Entropy Generation and Optimization for Laminar Forced Convection in a Rectangular Curved Duct with Longitudinal Ribs, *International Journal of Thermal Science, 45* (2006), 11, pp. 1113-1125
[20] Amani, E., Nobari, M. R. H., A Numerical Investigation of Entropy Generation in the Entrance Region of Curved Pipes at Constant Wall Temperature, *Energy, 36* (2011), 8, pp. 4909-4918
[21] Amani, E., Nobari, M. R. H., A Numerical Study of Entropy Generation in the Entrance Region of Curved Pipes, *Heat Transfer Engineering*, *31* (2010), 14, pp. 1203–1212
[22] Ishigaki, H., Fundamental Characteristics of Laminar Flows in a Rotating Curved Pipe, *Trans. JSME, 59-561-B* (1993), pp. 1494-1501
[23] Ishigaki, H., Laminar Flows in Rotating Curved Pipes, *Journal of Fluid Mechanics*, *329* (1996), Dec., pp. 373-388
[24] Patankar, S. V., *Numerical Heat Transfer and Fluid Flow*, Hemisphere, Washington, D.C., USA, 1980
[25] Hille, P., *et al*., The Development and Structure of Primary and Secondary Flow in a Curved Square Duct, *Journal of Fluid Mechanics*, *151* (1985), Feb., pp. 219-241
[26] Papadopoulos, P. K., Hatzikonstantinou, P. M., Thermally Developing Flow in Curved Square Ducts with Internal Fins, *Heat and Mass Transfer, 42* (2005), 1, pp. 30-38
[27] Hesselgreaves, J. E., Rationalisation of Second Law Analysis of Heat Exchangers, *International Journal of Heat Mass Transfer, 43* (2000), 22, 4189-4204

Paper submitted: June 6, 2012
Paper revised: January 28, 2013
Paper accepted: March 1, 2013